Hindawi Publishing Corporation
International Journal of Antennas and Propagation
Volume 2015, Article ID 683941, 7 pages
http://dx.doi.org/10.1155/2015/683941

Research Article

Measurements of Building Transmission Loss and Delay Spread at 2.5 GHz

L. H. Gonsioroski[1] and L. da Silva Mello[2]

[1]*Institute of Metrology, Quality and Technology (Inmetro), 20261-232 Rio de Janeiro, RJ, Brazil*
[2]*Pontifical Catholic University of Rio de Janeiro, 22451-900 Rio de Janeiro, RJ, Brazil*

Correspondence should be addressed to L. da Silva Mello; smello@cetuc.puc-rio.br

Received 25 April 2015; Accepted 15 June 2015

Academic Editor: Jose-Maria Molina-Garcia-Pardo

This paper presents the results of measurements of signal transmission loss at 2.5 GHz through 10 urban buildings. This allows the characterization of different types of buildings by effective attenuation constants and consideration of the contribution of the transmitted signal in microcell coverage predictions. Power delay profiles (PDPs) of the received signal were also measured and used to determine the time dispersion parameters of the channel, including the mean excess delay and the rms delay spread.

1. Introduction

Most empirical and semiempirical propagation models used to predict coverage by wireless systems only consider reflection, diffraction, and scattering effects. However, the component of the signal that is transmitted through buildings can be significant in some cases, particularly for microcells with base stations positioned below rooftops to provide coverage at street level [1–3].

Propagation studies on the transmission of radio waves through buildings were developed by Horikoshi et al. [2] and Risk [3]. They concluded that most urban propagation prediction models underestimate the field strength behind buildings by neglecting the contribution of the wave transmitted through the building structure.

de Jong et al. [4] used ray tracing techniques and experimental data to develop a semiempirical model that considers the contribution of transmission through buildings and have shown that it improves the coverage prediction in urban microcells. In their model, the transmission effect is characterized by an effective attenuation constant α_b, which was obtained for 20 different types of buildings by transmitting a 1.9 GHz signal with an antenna located in front of the buildings and a few meters above the street level and receiving the signal with a mobile unit moving slowly along a straight path behind the buildings. Although extensive in terms of the types of buildings found in The Netherlands, it is limited to the 1.9 GHz band. Additionally, construction characteristics of buildings vary in different part of the world due to local climate and regulations.

This paper presents results of measurements of transmission loss through buildings at 2.5 GHz. The 2.5 GHz frequency band became of particular interest because it was assigned to 4G LTE mobile systems. The measurements were performed in Rio de Janeiro, Brazil, on 10 buildings of 5 different types. Values for the specific attenuation, defined in the Jong model, were obtained for each building. The measurements confirmed that, behind the buildings, the contribution of a transmitted signal is not negligible when compared to the reflected and diffracted signals.

Wideband characterization of the channel was also performed, to provide the time dispersion parameters of the received signal. An OFDM channel sounder was used for the measurement of power delay profiles (PDPs) of the received signal, from which the mean excess delay and rms delay spread were obtained, as well as the cumulative probability distributions (CDFs) of the delay spread and the number of received multipath components.

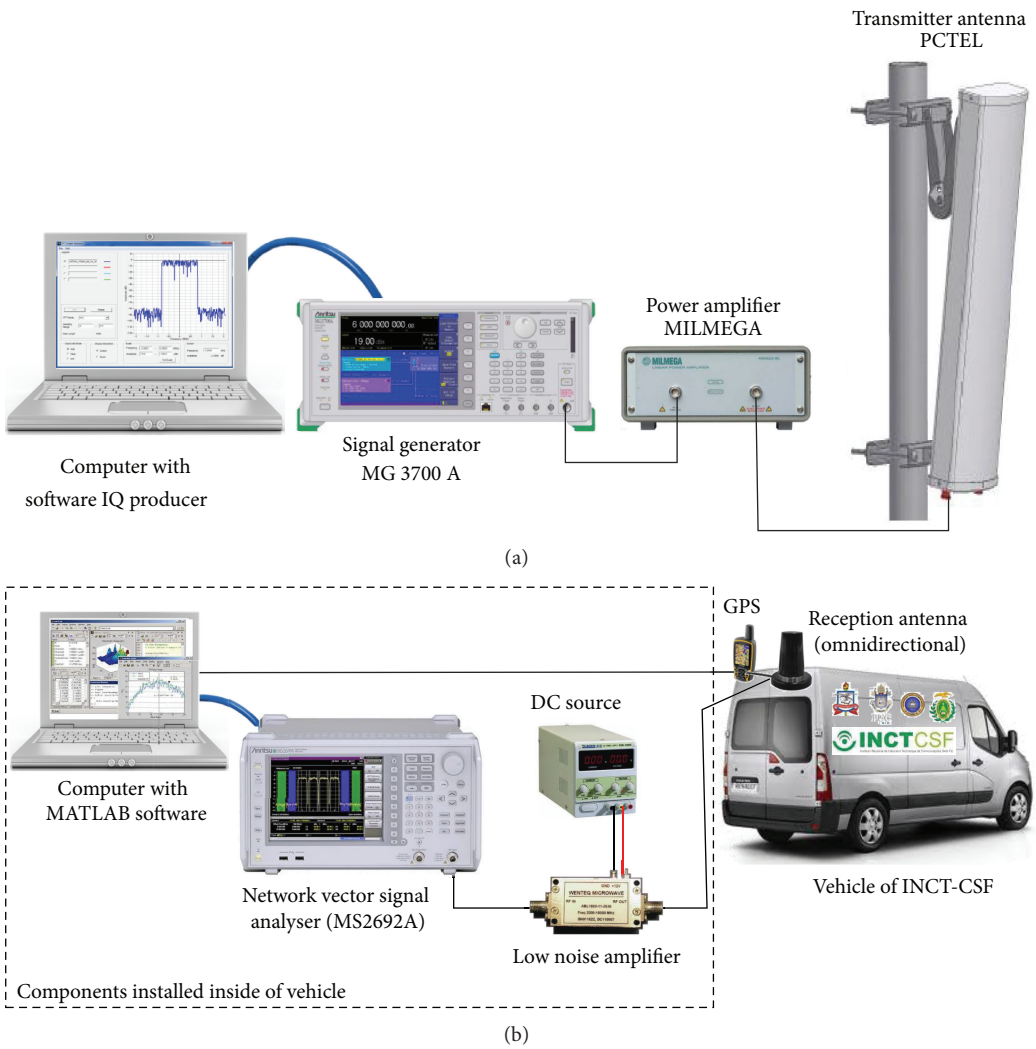

Figure 1: (a) Transmission setup; (b) reception setup.

2. Measurements Setup

A wideband channel sounder using the multicarrier technique [5] was employed. The measurements setup is shown in Figure 1. The transmission setup includes a vector signal generator ANRITSU MG3710A with an output power of −15 dBm, a power amplifier with 47 dB gain, cables and connectors with losses of 4.3 dB, and a vertically polarized sector antenna with 16 dBi gain and 90° horizontal beamwidth. To guarantee operation in the linear region of the amplifier, the output power of the signal generator was set to −15 dBm, resulting in a maximum EIRP of 43.7 dBm. The multicarrier OFDM signal parameters are presented in Table 1.

The transmitting antenna was positioned on one side of each building under test, at a height of 3-4 m, typical for base station configuration in urban microcells. The signal transmitted through and around the building is captured by a mobile receiving system moving with a constant speed of approximately 8 km/h along a linear path on the opposite side of the building, as shown in Figure 2.

Table 1: Parameters of the OFDM test signal.

Parameter	Value	Measurement unit
Channel bandwidth [BW]	20	MHz
FFT size [NFFT]	1024	Samples
Sampling factor	2	—
Sampling rate	50	Samples/second
Number of used carriers [N_{used}]	800	Carriers
PN length	1023	Bits
Cyclic prefix [CP]	1/16	Samples

The reception setup consists of an omnidirectional antenna with 2 dBi of gain, a low noise amplifier with 33 dB of gain, a vector signal analyzer (MS2692A), a GPS, and a laptop computer.

Figure 3 shows an example of the received power measurements for one building. The solid line corresponds to measurements in the diffraction region and the solid line with

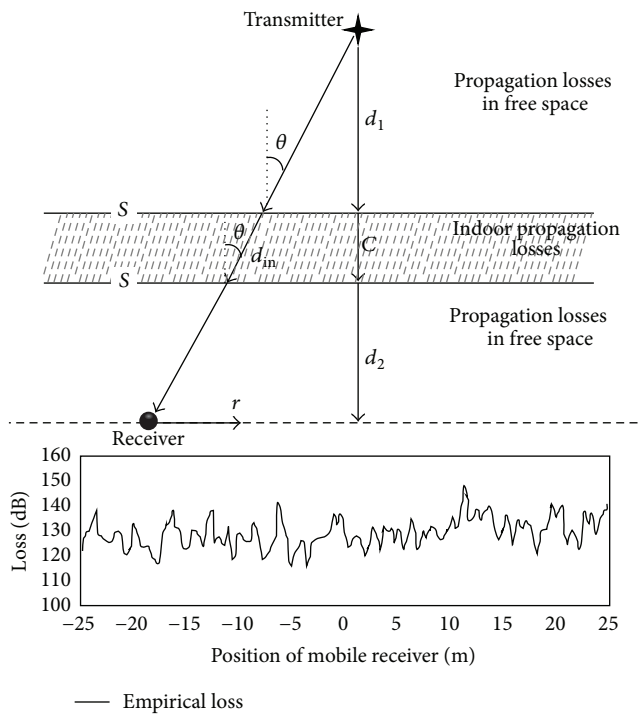

Figure 2: Measurements procedure.

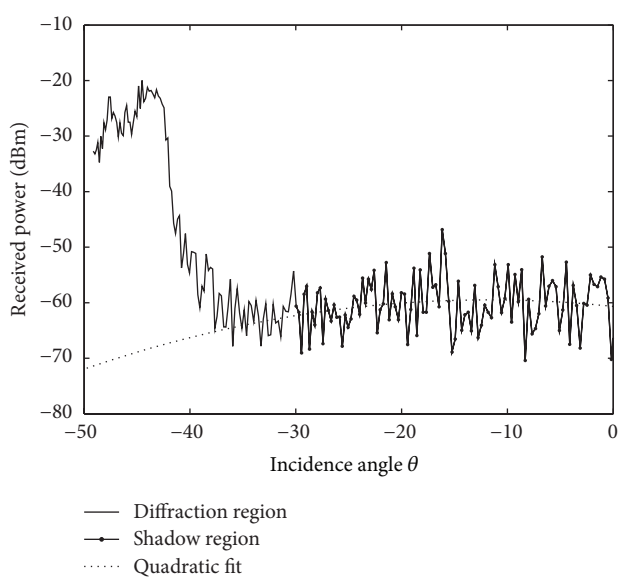

Figure 3: Received power versus incidence angle of building 3.

markers corresponds to measurements in the shadow region of the building.

3. Building Transmission Loss

3.1. The Jong Building Transmission Model. The transmission loss through a building depends on the penetration and exit losses through the external walls and also on the transmissions, reflections, and diffractions in internal walls, furniture, and other objects inside the building. The accurate prediction of the transmission loss would require a detailed description of the interior of the building, including electrical characteristics of materials; that is not practical. A simplified building transmission model was proposed by de Jong et al. [4], in which the building interior is treated as a homogeneous medium with an effective attenuation factor α_b that can be measured for different types of buildings. The external walls are modeled as thin planar slabs with complex relative permittivity ε_r. The building entry and exit losses are given by the Fresnel transmission coefficient. For simplicity, the losses inside the walls are accounted for by the effective attenuation factor, which also includes the losses in the building interior. The total building transmission loss is equal to the following [4]:

$$L_T = \alpha_b \cdot d_{\text{in}} - 40\log_{10}(T_s), \tag{1}$$

where α_b is the effective attenuation constant, d_{in} is the length of the straight path inside the building, and T_s is the Fresnel transmission coefficient given by the following [1]:

$$T_s = \sqrt{1 - |R_s|^2},$$
$$R_s = \frac{\cos\theta - \sqrt{\varepsilon_r - \sin^2\theta}}{\cos\theta + \sqrt{\varepsilon_r - \sin^2\theta}}, \tag{2}$$

where ε_r is the complex relative permittivity of the external wall and θ is the incidence angle. A permittivity equal to 5 was shown to be an optimum choice in two independent studies [6] and will be used in the following.

3.2. Effective Attenuation Measurements. The 10 different types of buildings were classified into four categories: residential buildings, office buildings, research laboratories, and university gymnasium. The buildings' characteristics are presented in Table 2.

The transmission loss (L_T) is measured as the difference between the effective isotropic transmitted power (EIRP) and the received power (P_R) plus the free space losses calculated for the paths between the transmitter and the building entry wall (at a distance d_t from the transmitter) and between the building exit wall and the receiver (at a distance d_r from the receiver). It is given by

$$L_T = \text{EIRP} - \left[P_R + 32.4 + 20\log f + 20\log(d_t + d_r)\right]. \tag{3}$$

The effective attenuation constant α_b (dB/m), associated with the losses due to the propagation inside the building, can be obtained for each point along the receiver path as

$$\alpha_b = \frac{L_T + 40\log(T_s)}{d_{\text{in}}}, \tag{4}$$

where d_{in} (m) is the path length inside the building.

The measured values of α_b show variations depending on the measurement position, due to the random distribution

Table 2: Effective attenuation constant for different types of buildings.

Buildings	Type of external walls	Building thickness (m)	Average transmission loss L_T (dB)	Average value of α_b (dB/m)	Standard deviation of α_b (dB/m)
Residential buildings Type A					
Building 3	Bricks and glass windows	56.46	46	1.16	0.22
Building 5	Bricks and glass windows	32.30	29	1.06	0.15
Residential buildings Type B					
Building 4	Brick walls coated with ceramic, balconies, doors, and glass windows	68.64	35	1.88	0.24
Building 6	Brick walls coated with ceramic, balconies, doors, and glass windows	46.93	31	1.46	0.22
University gymnasium					
Building 2	Reinforced concrete walls and brick and cast walls for ventilation	45.51	37	1.17	0.10
Office buildings					
Building 1	Bricks, windows, and wooden doors	61.54	21	2.71	0.28
Building 9	Bricks and wood windows	25.44	13	1.80	0.40
Research laboratory					
Building 7	Bricks and glass windows	39.04	37	0.95	0.20
Building 8	Bricks and glass windows	30.66	28	0.98	0.26
Building 10	Bricks and glass windows	29.86	20	1.30	0.41

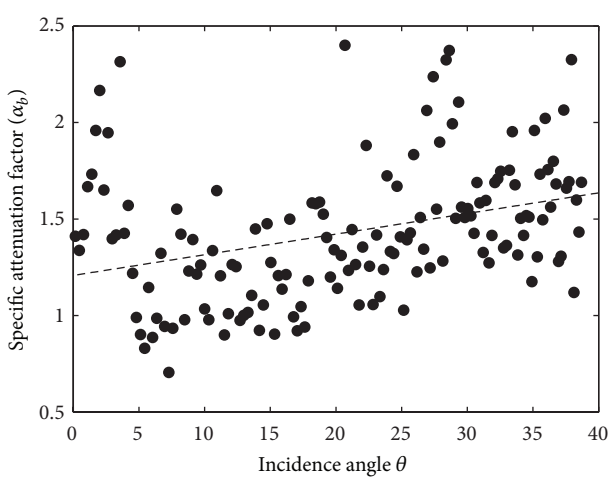

Figure 4: Specific attenuation factor versus building incidence angle, building 10.

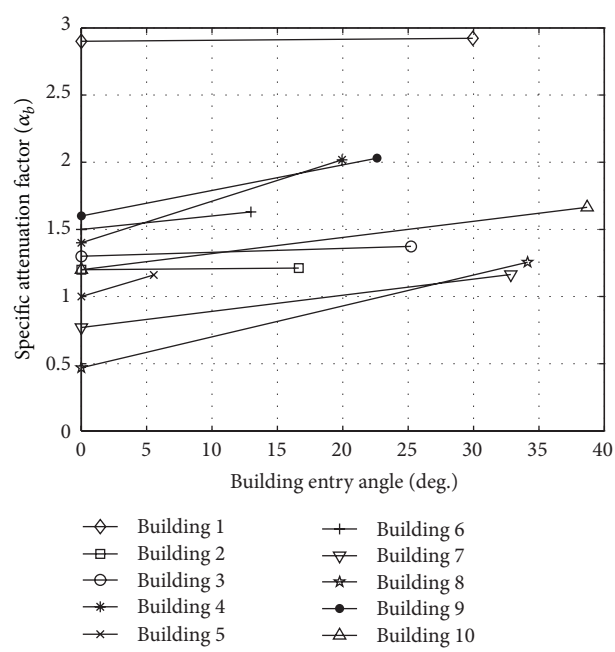

Figure 5: Linear approximations of α_b for all measurement sites.

of obstacles in the propagation path inside the building. Figure 4 shows the results for building 10, as an example. These variations show the trend of a slight increase of the attenuation coefficient with the angle of incidence, as the probability of finding obstacles increases with the path length inside the building that is also increased. Figure 5 shows the trend lines for all buildings.

Table 2 shows the average values and standard deviation of α_b for each building. The average value of the transmission loss is also shown.

The residential buildings of type A have external brick walls with glass windows, 4 to 5 floors and few apartments per floor. Residential buildings of type B have external brick walls coated with ceramic, balconies with glass doors and glass windows, 10 to 12 floors, and more apartments per floor. This may explain the larger values of the attenuation constant, as the buildings have more internal walls and furniture. The office buildings show the largest attenuation constant values, as they have an even larger number of internal walls dividing the internal space in small offices. Smaller attenuation constants were measured for the research laboratories and the university gymnasium, with larger internal spaces. Buildings 5, 6, and 9 seem to be externally similar to some buildings considered in Jong's work. The other buildings have different architectural characteristics.

The standard deviations of the measured values of the effective attenuation constant are, in almost all cases, small enough to justify Jong's approximation that considers the interior of the building as homogeneous media. The higher values of standard deviation obtained for buildings 9 and 10 are probably due to the more complex interior structures of these buildings, making the approximation less accurate.

4. Wideband Characterization

The wideband behavior of the channel can be characterized by the power delay profiles of the signals transmitted through the buildings. The OFDM multicarrier sounding technique [5, 7] was employed, in which a known OFDM signal is generated, amplified, and transmitted through the channel. At the receiver, the method of cross-correlation of the cyclic prefix is used to provide synchronization and the correct identification of the symbols. The signal is filtered, and its autocorrelation provides the power delay profile (PDP). An example of PDP obtained using this technique is shown in Figure 6, corresponding to measurements of the signal transmitted through building 5.

The measured power delay profiles contain spurious components due to the noise in the channel. The real multipath components can be separated from the noise components in the postprocessing step using the CFAR technique [8].

After being filtered, the power delay profiles are processed to provide the average excess delay and RMS delay spread, parameters defined in ITU-R [9] to characterize the channel dispersion.

The values obtained for these parameters, in the deep shadow region of six of the buildings considered in this study, are shown in Table 3, including the mean value, standard deviation, and maximum and minimum values measured. Following Recommendation ITU-R 1411-6 [9], for the rms delay spread, the median value and the value not exceeded for 95% of the cases are also presented.

Almost all the buildings considered in the measurements are surrounded by other buildings, assuring that the contribution to the received field of components reflected by the environment could be neglected, so that (3) is a valid approximation. It can be noted that the mean values of average delay and rms delay spread are of the same order for all buildings, except for building 4. This building is relatively isolated and surrounded by vegetation, and the higher values of delay spread in this case may be due to components reflected by the environment.

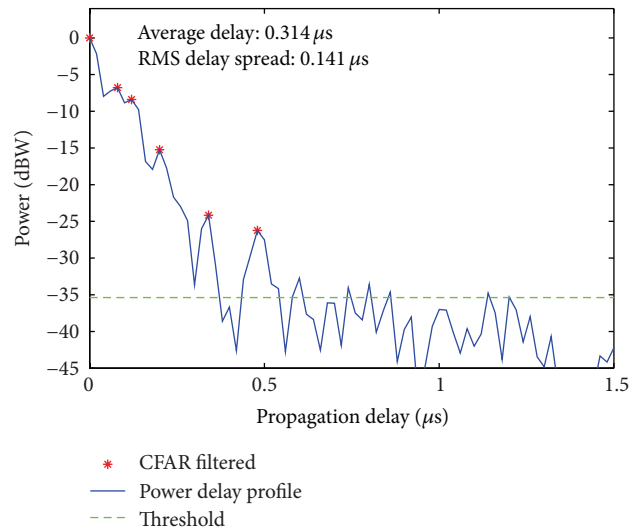

Figure 6: Measured power delay profile for building 5.

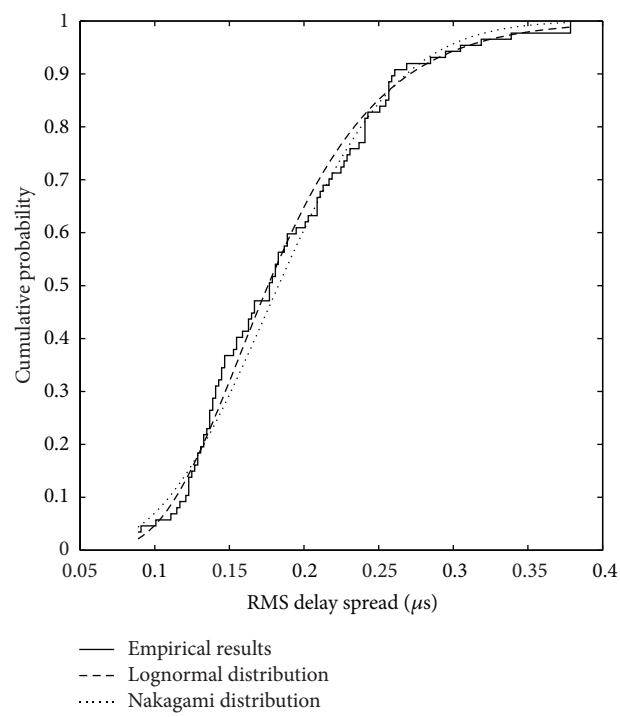

Figure 7: CDF of RMS delay spread for building 5.

The cumulative distribution functions of the rms delay spread and the number of multipath components were also obtained. Examples are shown in Figures 7 and 8. The number of multipath components is the number of identifiable peaks in the measured power delay profiles, as indicated in Figure 6.

Table 3 shows the parameters of the distributions that best fitted the CDF of the rms delay spread for each building.

Table 3: Statistical parameters of multipath time dispersion.

	Multipath delay (ns)				RMS delay spread (ns)						CDF of RMS delay spread			CDF of number of components
	Mean	Std.	Min	Max	Mean	Std.	Min	Max	50%	95%	Best fit	Parameters		Poisson parameter (λ)
Building 1	461.1	112.5	200.1	797.6	198.1	70.8	29.8	393.5	198.5	339.2	Nakagami	$(m) = 2.35$	$(\Omega) = 0.05$	7.36
Building 2	472.4	92.3	270.0	896.7	198.6	49.5	93.7	466.5	201.0	279.4	Weibull	$(\lambda) = 0.21$	$(\alpha) = 4.01$	7.47
Building 3	450.1	90.1	189.1	753.4	195.7	54.4	39.0	362.8	199.6	268.5	Weibull	$(\lambda) = 0.21$	$(\alpha) = 3.94$	7.75
Building 4	637.8	143.0	361.6	975.3	314.1	101.7	98.9	600.3	303.3	522.9	Nakagami	$(m) = 2.46$	$(\Omega) = 0.11$	10.19
Building 5	441.2	89.6	259.7	693.6	186.1	64.2	88.9	378.5	176.4	303.9	Lognormal	$(\mu) = 0.18$	$(\sigma) = 0.06$	6.77
Building 6	460.5	142.4	191.2	1083	207.2	94.7	64.1	656.4	203.7	349.6	Nakagami	$(m) = 1.48$	$(\Omega) = 0.05$	6.87

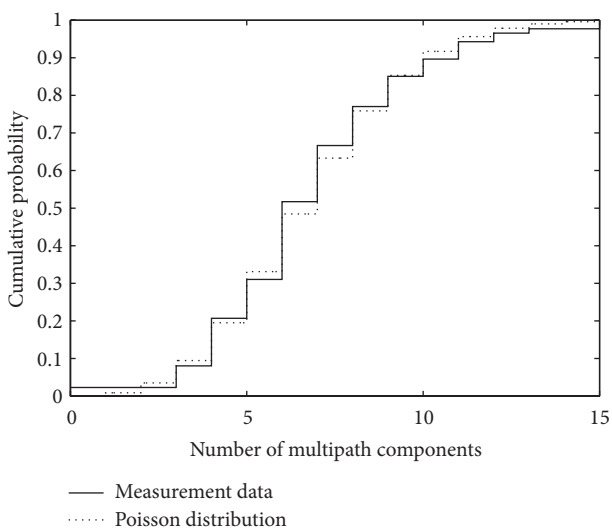

Figure 8: CDF of the number of multipath components for building 5.

The CDFs of the multipath components are well fitted by a Poisson distribution in all cases.

5. Conclusions

Based on field measurements at 2.5 GHz, the effective attenuation constant for transmission through buildings in urban environments, as defined in the Jong model, was obtained for 10 different buildings. The results show that, despite the high attenuation, the contribution of the transmitted field is significant and should be considered when estimating the coverage of small cells in dense urban regions.

Average values of the attenuation constant varied, depending on the type of building, from approximately 1 dB/m, for research laboratories and residential buildings with few internal walls, to 2.7 dB/m, for office buildings with many internal walls.

For six of the buildings, the mean values of the multipath delay and the rms delay spread of the signals transmitted through the buildings were also obtained, to characterize the wideband behavior of the channel. Depending on the type of building, the CDF of the rms delay spread is best fitted by a Nakagami or a Weibull distribution. In one single case, the lognormal distribution provided the best fit. For all buildings, the number of multipath components follows a Poisson distribution.

Conflict of Interests

The authors declare that there is no conflict of interests regarding the publication of this paper.

Acknowledgments

This work was supported by the National Institute Metrology, Quality and Technology (Inmetro), under the Pronametro and Prometro Programs, and by CNPq (National Research Council, Brazil), under Covenant 573939/2008-0 (INCT-CSF).

References

[1] Y. L. C. de Jong, *Measurement and modeling of radiowave propagation in urban microcells [Ph.D. thesis]*, Eindhoven University of Technology, Eindhoven, The Netherlands, 2001.

[2] J. Horikoshi, K. Tanaka, and T. Morinaga, "1.2 GHz band wave propagation measurements in concrete building for indoor radio communications," *IEEE Transactions on Vehicular Technology*, vol. 35, no. 4, pp. 146–152, 1986.

[3] K. Risk, *Propagation in microcellular and small cell urban environment [Ph.D. thesis]*, Ecole Polytechnique Fkdkrale de Lausanne, Lausanne, Switzerland, 1997.

[4] Y. L. C. de Jong, M. H. J. L. Koelen, and M. H. A. J. Herben, "A building-transmission model for improved propagation prediction in urban microcells," *IEEE Transactions on Vehicular Technology*, vol. 53, no. 2, pp. 490–502, 2004.

[5] G. Acosta-Marum, *Measurements, modeling, and OFDM synchronization for the wideband mobile-to-mobile channel [Ph.D. thesis]*, Georgia Institute of Technology, Atlanta, Ga, USA, 2007.

[6] G. E. Athanasiadou and A. R. Nix, "Investigation into the sensitivity of the power predictions of a microcellular ray tracing propagation model," *IEEE Transactions on Vehicular Technology*, vol. 49, no. 4, pp. 1140–1151, 2000.

[7] R. M. L. Silva, G. L. Siqueira, L. H. Gonsioroski, and C. R. V. Ron, "Comparison between OFDM and STDCC mobile channel sounders at 3.5 GHz," *Journal of Microwaves, Optoelectronics and Electromagnetic Applications*, vol. 12, no. 1, 2013.

[8] E. S. Sousa, V. M. Jovanovic, and C. Daigneault, "Delay spread measurements for the digital cellular channel in Toronto," *IEEE Transactions on Vehicular Technology*, vol. 43, no. 4, pp. 837–847, 1994.

[9] ITU, "Multipath propagation and parameterization of its characteristics," Recommendation ITU-R P.1407-5, International Telecommunication Union, 2013.